Research Square

Preprints are preliminary reports that have not undergone peer review.
They should not be considered conclusive, used to inform clinical practice,
or referenced by the media as validated information.

Assessment of natural radionuclide distribution and radiological hazards in Egyptian soil using gamma-ray spectroscopy and evaluating with Monte Carlo simulation and Artificial Neural Network

A. F. Saad

afsaad@zu.edu.eg

Zagazig University

M. Al-Abyad

Atomic Energy Authority

Amany T. Gendya

Zagazig University

E. M. Sedqy

Sinai University

Mahmmoud A. Ibraheim

Zagazig University

Mohammed Elywa

Zagazig University

Article

Keywords: Soil, HPGe gamma-ray spectrometer, Monte Carlo simulation, Artificial Neural Network, Radiological parameters, Radium equivalent content, Gamma absorbed dose, External hazard index

Posted Date: August 6th, 2026

DOI: https://doi.org/10.21203/rs.3.rs-10264372/v1

License: This work is licensed under a Creative Commons Attribution 4.0 International License.
Read Full License

Additional Declarations: No competing interests reported.

Assessment of natural radionuclide distribution and radiological hazards in Egyptian soil using gamma-ray spectroscopy and evaluating with Monte Carlo simulation and Artificial Neural Network

A.F. Saad[*, a], M. Al-Abyad [b], Amany T. Gendya [a], E.M. Sedqy [c], Mahmmoud A. Ibraheim [a], Mohammed Elywa[a]

[a)] *Physics Department, Faculty of Science, Zagazig University, P.O. 44519, Zagazig, Egypt*

[b)] *Experimental Nuclear Physics Department (Cyclotron Facility), Nuclear Research Centre, Atomic Energy Authority, B.O. 13759, Cairo, Egypt*

[c)]*Basic Science Department, Faculty of Engineering, Sinai University, El-Arish, Egypt*

Abstract

The activity concentration of naturally occurring radioactive nuclides ^{226}Ra, ^{238}U, ^{232}Th, and ^{40}K from soil samples collected from two cities: 10th of Ramadan and Zagazig, located in the Sharqia governorate in the eastern of Nile Delta, Egypt were measured using a high resolution HPGe gamma-ray spectrometer. The present study also uses Monte Carlo Simulation (MCS) and an Artificial Neural Network (ANN) model to perform theoretical calculations of the associated radiological hazard parameters for soil samples collected from these two cities and compared them with the measured experimental data. The use of artificial neural networks allows for taking advantage of large amounts of data at a very low computational cost, and the use of Monte Carlo simulation can produce predictions of the levels of radioactive materials and their future health risks at the regional level. The theoretical calculations based on the Monte Carlo simulation and Artificial Neural Network (ANN) model for these radiological parameters of soil samples are in excellent agreement with the experimental results. The findings demonstrate that the activity concentration of radioactive nuclides and radium equivalent content, gamma absorbed dose, annual effective gamma dose rate and external hazard index in soil samples collected from Zagazig are about two times higher than those the values of samples collected from 10th of Ramadan. Overall, the soil samples from both cities are almost below the recommended level issued by the international committees on the effects of atomic radiation.

Keywords: Soil; HPGe gamma-ray spectrometer; Monte Carlo simulation; Artificial Neural Network; Radiological parameters; Radium equivalent content; Gamma absorbed dose; External hazard index

* Corresponding author at: Physics Department, Faculty of Science, Zagazig University, 44519 Zagazig, Egypt. Tel.: +20 55 2303252; Fax: +20 55 2308213, Mobile: +20 1016746496; 12253074

E-mail address: afsaad@zu.edu.eg , abdallah.saad2256@gmail.com, abdallahsaad56@hotmail.com. (A.F. Saad).

1. Introduction

The natural radioactivity present in all types of soil is the main source of ionizing radiation exposure for humans[1,2]. In the Earth's crust, radioactive nuclides are found in the decay chains of uranium and thorium at varying concentrations[3].While radioactive nuclei such as radium (^{226}Ra), radon (^{222}Rn), and bismuth (^{214}Bi) are produced in the decay series of uranium (^{238}U), other radioactive nuclei including actinium (^{228}Ac), bismuth (^{212}Bi), and lead (^{212}Pb) are found in the decay series of thorium (^{232}Th)[4] . Additionally, the naturally occurring radioactive isotope ^{40}K is present in virtually all soil types because potassium is an essential constituent of many rock-forming minerals[1]. These radionuclides occur naturally in geological materials such as rocks, granite, sand, cement, and plaster[2]. Knowledge of ionizing radiation levels in soil, which are directly related to the concentrations of naturally occurring radionuclides, is essential for assessing human radiation exposure, particularly because people spend approximately 80% of their time indoors[1]. Human exposure occurs through two principal pathways: (i) external exposure to gamma radiation emitted by ^{40}K, ^{238}U, ^{232}Th, and their decay products, resulting in whole-body irradiation, and (ii) internal exposure due to inhalation of ^{222}Rn and its short-lived progeny, which deposit in the respiratory tract and significantly contribute to the effective radiation dose received by humans[1,5].

All raw materials, including soils and rocks used in the production of building materials worldwide, naturally contain varying concentrations of primordial radionuclides. Consequently, humans are continuously exposed to ionizing radiation from both outdoor (external) and indoor (internal) sources. External exposure primarily results from terrestrial gamma radiation emitted

during the decay of naturally occurring radionuclides, particularly those belonging to the Uranium-238 decay series, Thorium-232 decay series, and Potassium-40. Within the uranium decay series, Radium-226 is considered the most radiologically significant progeny because it is the immediate precursor of Radon-222 and contributes substantially to terrestrial gamma dose rates; therefore, ^{226}Ra activity concentration is commonly used as a surrogate for the ^{238}U series in environmental radioactivity assessments[1,2]. Internal exposure arises from gamma radiation emitted by naturally occurring radionuclides incorporated into building materials, as well as from the inhalation of radon-222 and its short-lived progeny, particularly Polonium-218 and Polonium-214. The concentration and migration of radon depend strongly on geological conditions, soil permeability, and the presence of cracks and pores in building structures, allowing the gas to accumulate indoors and become a major contributor to the annual effective radiation dose received by the public [6-8].

HPGe gamma-ray spectrometer, as the finest tool with a high resolution, has been used in the study of gamma-ray detection of natural radioactivity in soil. In addition, Monte Carlo Simulation (MCS) and an Artificial Neural Network (ANN) model as a powerful approach for accurately modeling assessing the natural radio-nuclide contents, radiation risks and monitoring environmental radiation are also used.

Recent advances in computational modeling have significantly improved the assessment of environmental radioactivity and radiological risk. Monte Carlo simulation (MCS) has become one of the most reliable stochastic techniques for propagating uncertainties in radiological calculations because it generates thousands of random realizations of input variables, allowing realistic estimation of uncertainty ranges and confidence intervals[9,10]. In parallel, Artificial Intelligence (AI), particularly Artificial Neural Network (ANN) models, has emerged as an efficient predictive tool capable of modeling highly nonlinear relationships between radionuclide concentrations and radiological hazard indices without requiring explicit mathematical formulations[11-13]. The integration of Monte Carlo simulation with ANN models provides a powerful hybrid framework

that combines uncertainty quantification with data-driven prediction, leading to improved accuracy, computational efficiency, and reliability in environmental radiation assessment. Such integrated approaches have recently been adopted in radioecological studies for predicting radionuclide distributions, estimating radiation exposure, supporting environmental monitoring, and assisting decision-making in radiation protection, environmental risk assessment, and nuclear safety[14].

The work aims to evaluate natural radioactivity impact from soil samples collected from two cities: ^{10}th of Ramadan and Zagazig, located in the Sharqia governorate in the eastern of Nile Delta, Egypt, assessing the radiation risks to the residents of these areas. This study seeks to achieve a concise comprehension of the correlation between natural radioactivity emitted from soil and the associated radiological hazards, employing measured experimental reasoning to establish the form of the radioactivity concentrations in soil. Subsequently, the measured natural radio-nuclide contents are utilized to ascertain the radiation risks to the people living in these areas. This Monte Carlo Simulation (MCS) approach, incorporating the Artificial Neural Network (ANN) model is then employed to predict the natural radio-nuclide contents in soil of both two cities and the dosimetric and hazard parameters, with a specific focus on all measured hazard parameters.

2. Geography and geology of the study area

The studied area included the cities of ^{10}th of Ramadan and Zagazig, both of which are located in the Sharqia Governorate in the eastern part of Egypt. ^{10}th of Ramadan is the first generation of the new urban community and is considered the most important industrial city in Egypt. It was established in 1977 in an attempt to attract foreign and local investments. It is located on the Cairo–Ismailia Desert Road, 46 km from Cairo and 20 km from Belbis City, at the coordinates 30.18° North and 31.44° East, as shown in Figure 1a. The city of ^{10}th of Ramadan is situated in a plain area surrounded by sand on all sides. The soil of the ^{10}th of Ramadan area consists

of classified sandy soil containing lenses of clay and shale from the modern era. Zagazig is a city in the Egyptian Delta, situated in the eastern region of the Nile Delta. It is the capital of the Sharqia Governorate. Zagazig is located on the Moais Canal, a small branch of the Nile River, between 30.59° north latitude and 31.50° east longitude as shown in Fig. 1b. The soil of Zagazig is characterized by its high clay content and is sometimes derived from ancient Nile branches, with shallow water present. In general, the soils surrounding Zagazig face significant challenges due to salinity and clay.

3. Experimental methods and set-up

3.1 Collection of soil samples

Forty samples of soil were collected from 10^{th} of Ramadan and Zagazig, 25 from 10^{th} of Ramadan and 15 from Zagazig as shown in Fig. 1. The collected samples were dried in an oven at a temperature 105 ± 1 ºC for 24 h to remove moisture and then sieved through a 1-mm-mesh sieve.

3.2 Radiometric analysis experimental set-up

A low-level gamma ray spectrometric set up at the Experimental Nuclear Physics Department, Nuclear Research Centre, Atomic Energy Authority, was used for the estimation of ^{226}Ra ^{238}U, ^{232}Th and ^{40}K. The homogenized samples, each having a volume of 500 cc, were put into a 1 l size well sealed containers (similar to those of the standard), stored a month to get a secular equilibrium and counted with high-purity germanium (HPGe) gamma-ray spectroscopy (Canberra, 70 % relative efficiency, 2.3 keV resolution at 1332.5 keV of ^{60}Co) coupled with a computer-based multichannel analyzer card system, which could determine the photo-peak-area of γ-ray spectra by using the GENIE-2000 (Canberra) computer program. The detection efficiency versus energy curve of the HPGe gamma-ray detector for the counting distance was determined using a set of standard point sources such as ^{60}Co, ^{133}Ba, ^{137}Cs and ^{152}Eu at different distances (47.5, 30, 17.5 and 8 cm) from the detector[15-17]. The measuring times were chosen based on the activity and the half-life of each radioactive isotope.

3.2.1 Radium equivalent activity

Radiation exposure is defined in terms of activity of radium equivalent content (Ra_{eq}) in Bq kg^{-1} to compare the specific activity of materials containing different amounts of ^{238}U, ^{232}Th and ^{40}K. Radium equivalent content Ra_{eq} is calculated through the following expression[18]:

$$\mathbf{Ra_{eq} = A_U + 1.43\, A_{Th} + 0.07 A_K} \quad (1)$$

Where A_U, A_{Th} and A_K are the activity concentrations of ^{238}U, ^{232}Th and ^{40}K in Bqkg^{-1}, respectively. In the above equation for defining $\mathbf{Ra_{eq}}$ activity it has been assumed that the same gamma dose rate is produced by 370 Bq kg^{-1} of ^{238}U or 259 Bqkg^{-1} of ^{232}Th or 4810 Bq kg^{-1} of ^{40}K. There is a variation in radium-equivalent activities in different types of soil. The results may be significant from the perspective of selecting suitable soil for agricultural purposes and its use in brick manufacturing.

3.2.2 Annual effective gamma dose

The absorbed gamma dose rates (D) in air at 1m above the ground surface for the uniform distribution of radio nuclides (^{232}Th, ^{238}U & ^{40}K) are calculated on the basis of guiding principle as mentioned by reference[1]. The dose conversion factors for converting the activity concentrations of ^{238}U, ^{232}Th and ^{40}K into doses (nGyh^{-1} per Bq kg^{-1}). Consequently, the absorbed gamma dose rate is as follows:

$$D = (0.462\, A_U + 0.604\, A_{Th} + 0.0417\, A_K)\ nGyh^{-1} \quad (2)$$

The annual effective dose rates (mSvyr^{-1}) were estimated by using the conversion coefficient from absorbed dose in air to effective dose (0.7 Sv/Gy) and proposed outdoor occupancy factor (0.2)[1] as the follows:

$$\text{Effective dose rate (mSv yr}^{-1}) = \text{Dose rate (nGyh}^{-1}) \times 8760\ h \times 0.2 \times 0.7\ Sv\ Gy^{-1} \times 10^{-6} \quad (3)$$

3.2.3 External Hazard Index

Krieger,1981[19], proposed the following relation for external hazard index H_{ex} estimation as the following relation:

$$H_{ex} = \frac{A_U}{370} + \frac{A_{Th}}{259} + \frac{A_K}{4810} \leq 1 \quad (4)$$

This standard only takes into account the external exposure risk from gamma rays and complies with the maximum radium equivalent of 370 Bq kg^{-1} of material.

4. Theoretical background on Mont Carlo Simulation and an Artificial Neural Network model

To calculate the radiological parameters and the associated health risk parameters, MCS was used to account for uncertainty and variability in several parameters. In order to do the sensitivity analysis, 10,000 iterations were run using the Oracle Crystal Ball programme for MCS. From their fitted distribution, MCS selected the parameter values that allowed them to assess exposure risk and point value. Variations in MCS output, which might be attributed to changes in the input data, were examined using SA. Developing an Artificial Neural Network Model, it needs designing and developing for complex systems, it can be difficult to determine the relationship between target variables and inputs. In such cases, artificial neural networks offer a unique and in-depth solution to address these problems. Prediction is one of the most common applications of this technique. The basic steps in designing and developing artificial neural network models include selecting appropriate inputs, defining the network architecture, processing and segmenting the available input data, selecting the network structure, setting performance criteria, training, testing, and validating[20,21].

5. Results

5.1. Results of radiometric analysis using gamma-ray spectroscopy

Tables 1 and 2 present the results of the measurements of naturally radioactive concentration levels in $Bqkg^{-1}$ for ^{226}Ra, ^{238}U, ^{232}Th and ^{40}K for some radionuclides of soil samples collected from different sites in 10^{th} of Ramadan and Zagazig were measured by using HPGe gamma ray spectrometry. In addition to estimated parameters such as radium equivalent content ($Bqkg^{-1}$), gamma absorbed dose (nGy/h), annual effective gamma dose rate ($\mu Svyr^{-1}$) and external hazard index (Bq/kg). The activity concentrations of each nuclide in these soil samples and the estimated parameters; radium equivalent content ($Bqkg^{-1}$), gamma absorbed dose (nGy/h), annual effective gamma dose rate ($\mu Svyr^{-1}$) and external hazard index (Bq/kg) are listed in both Tables 1 and 2. The comparison between variations of both cities (minimum, maximum, range and mean values) of concentrations of radionuclides (in Bq kg^{-1}) and radium equivalent content ($Bqkg^{-1}$), gamma absorbed dose (nGy/h), annual effective gamma dose rate ($\mu Svyr^{-1}$) and external hazard index (Bq/kg), in addition to the standard deviation (SD), as seen in Table 3. The activities of ^{226}Ra, ^{238}U, ^{232}Th and ^{40}K in the study samples of 10^{th} of Ramadan city varied from 5.6 ± 0.4, 11.1 ± 3.0, 6.8 ± 0.4, and to 99.3 ± 6.9 up to 11.9 ± 2.3, 53.2 ± 14.6, 14.1 ± 2.6 and to 181.6 ± 32.7 Bq kg^{-1}, while in the Zagazig samples varied from 13.8 ± 0.6, 15.7 ± 8.2, 20.0 ± 0.9 and to 305.7 ± 16.8 up to 21.4 ± 1.4, 52.4 ± 18.9, 28.2 ± 1.9 and to 498.0 ± 27.3 Bq kg^{-1}, respectively as shown in Table 3. The world average activity concentrations of ^{226}Ra, ^{238}U, ^{232}Th and ^{40}K are 35, 25.5, 30, and 400 Bq kg^{-1}, respectively[4]. Some concentrations of ^{238}U in six samples of 10^{th} of Ramadan city; Ash5, Ash8, Ash9, Ash12. Ash13 and Ash23; were considerably higher than the world average of 25.5 Bq kg^{-1}, in the same context, it was found that nine samples from the city of Zagazig; Z1, Z2, Z5, Z9, Z10, Z11, Z13, Z14 and Z15; were also higher than this world average [16]as shown in Tables 1 and 2. In Zagazig samples, numerous samples had high concentrations of ^{238}U (60 % of the Zagazig samples), and one sample in both cities, Ash9 and Z1, had double high value than the recommended normal world limit, in addition to four samples of Zagazig region had extremely high values above 40 Bq kg^{-1}. All samples collected from 10^{th} of Ramadan city had lower

concentrations of ^{40}K than the recommended normal world limit of 400 Bq kg^{-1}. While in the case of samples collected from Zagazig city, five samples had higher values of 498.0 ± 26.9, 443.4 ± 24.4, 451.1 ± 26.0, 457.8 ± 27.3 and 417.9 ± 23.1 Bq kg^{-1} than this world limit. These samples were collected from some regions of Zagazig city are considered as a high background radiation area of ^{238}U and ^{40}K. On the contrary, the Zagazig samples had low values of ^{226}Ra and ^{232}Th than the recommended normal world limit as seen in Table 2.

It can be seen that among all the samples in both cities, the values (minimum, maximum and mean) of radium equivalent content ($Bqkg^{-1}$), gamma absorbed dose (nGy/h), annual effective gamma dose rate ($\mu Svyr^{-1}$) and external hazard index (Bq/kg) for each sample from 10^{th} of Ramadan city given in Table 3 are about half of those obtained in Zagazig samples. It should be noted that the mean dose rate as computed from Eq. 2 for Zagazig samples is found to be less than 51 $nGyh^{-1}$, except two samples Z1 and Z2 are little bit more than 51 $nGyh^{-1}$, which is approximately similar the world average (51$nGyh^{-1}$) as reported by[22], whereas for 10^{th} of Ramadan samples it is found to be by far lesser than the world average (51$nGyh^{-1}$).

5.2. Results of Artificial Neural Network Performance and Monte Carlo Simulation

Fig. 2 (a) illustrates the architecture of the Artificial Neural Network (ANN)[20,21] developed in this study. The network consists of an input layer, multiple hidden layers, and an output layer designed to model the complex nonlinear relationships between radionuclide concentrations and radiological hazard parameters. The multilayer structure enhances the learning capability of the model and enables accurate prediction of the target variables. The ANN training performance in terms of the Mean Squared Error (MSE) versus training epochs as seen in Fig. 2 (b). The performance curve shows a continuous decrease in MSE throughout the training process until reaching its minimum value at epoch 1000. The best training performance achieved was approximately 1.1×10^{-7}, indicating excellent convergence and extremely small prediction errors.

Such a low MSE demonstrates the effectiveness of the ANN model in learning the underlying patterns of the dataset. Fig. 2 (c) shows the training of the artificial neural network, including the gradient, the damping factor (μ), and the validation checks. The gradient gradually decreased during training, indicating a successful reduction of the target function. The damping factor reached a very small value, reflecting stable optimization behavior, while the validation checks stayed constant without any major failures, suggesting that overfitting didn't happen and the network maintained good generalization ability. The regression analysis between the values predicted by the artificial neural network and the corresponding target values is shown in Figure 2 (d). The regression coefficient (R = 1) indicates an almost perfect correlation between the predicted and measured data. Moreover, the data points closely follow the ideal regression line, confirming the high predictive accuracy and reliability of the developed artificial neural network model. Fig. 2 (e) shows the correlation matrix between the radioactive activity concentrations of isotopes and the statistics calculated for radiation risks. The color scale shows different levels of correlation, with yellow areas indicating strong positive correlations and blue areas showing weak correlations. The matrix highlights strong relationships among most risk indicators, confirming that changes in isotope concentrations directly affect radiation risk parameters. Fig. 2 (f) shows the Monte Carlo simulation distribution of the radium equivalent activity (Ra_{eq}). The histogram displays a near-normal distribution with most values clustered around the mean. The relatively narrow spread indicates a low uncertainty in estimating Ra_{eq}. Moreover, all simulated values remain well below the internationally accepted limit of 370 Bq/kg, confirming the radiation safety of the examined samples. Fig. 2 (g) shows the Monte Carlo distribution of the absorbed dose rate. Like Ra_{eq}, the distribution is almost normal, with most of the simulated values clustered around the average dose rate. The limited spread of the distribution highlights the strength of the dose assessment and suggests that uncertainty in the radioactive isotope concentrations has only a minor impact on the estimated dose rates. The comparison between the actual and ANN-predicted dose rate values for

samples collected from both cities: ^{10}th Ramadan and Zagazig are shown in Figs, 2 (h and i), respectively. In both cases, the predicted values closely match the measured values, producing nearly linear relationships with minimal deviations. These results demonstrate the strong predictive capability of the ANN model and confirm its applicability for estimating radiological dose rates across different sampling locations.

Overall, the combined analyses of artificial neural networks and Monte Carlo simulation show excellent predictive performance, high model reliability, and strong robust uncertainty. The very low of mean square error (MSE) value, the near-perfect regression coefficient, and the stable Monte Carlo distributions all indicate that the developed methodology is effective in assessing radiation risks and monitoring environmental radiation.

5.3. Comparison of results between experimental measurement and the combined approach of Monte Carlo simulation and artificial neural network model

Table 4 shows a comparison between the measured and the simulated results using the Monte Carlo method for soil samples collected from the cities of Tenth of Ramadan and Zagazig. The results concerning the radioactive concentrations of ^{226}Ra, ^{238}U, ^{232}Th and ^{40}K and their associated radiological hazards due to naturally occurring radioactive materials (NORM) [6, 23,24] in soil using the gamma-ray spectroscopy method are in excellent agreement with the predicted theoretical results evaluated using Monte Carlo simulation (MCS) and an artificial neural network (ANN) model. While the predicted ^{238}U concentration (Bq kg^{-1}) assessed using the MCS and ANN model decreased significantly by more than two times compared to the measured sample for the city of Tench of Ramadan with an average squared error of 0.476 (%), in the case of the city of Zagazig, it decreased to almost one-sixth with an average squared error of 0.159(%). On the other hand, the mean squared error for the concentrations of the other three radioactive isotopes ^{226}Ra, ^{232}Th and ^{40}K ranges between 0.002 and 0.061 (%) in ^{10}th of Ramadan City, and between 0.006 and 0.035

(%) in Zagazig. Similarly, the mean squared error for the annual effective dose, radium equivalent content, external hazard index, internal hazard index, annual effective dose (external and internal), and gamma index (I gamma) ranges between 0.037 and 0.42 (%) in ^{10}th of Ramadan City, and between 0.012 and 0.015 (%) in Zagazig.

Discussion and conclusion

In this study, we investigated the naturally occurring radioactive materials (NORM) in soil using the gamma-ray spectroscopy technique and also using a combination of artificial neural networks and Monte Carlo simulation.to assess radioactive concentrations of ^{226}Ra, ^{238}U, ^{232}Th and ^{40}K and their associated radiological hazards[25]. Our computational results demonstrate the effectiveness of this integrated approach and its impact on improving the efficiency of radioactivity analysis compared with the experimental data. It should be noted that some concentrations of ^{238}U in both cities, 10th of Ramadan and Zagazig, were considerably higher than the world average of 25.5 Bq kg^{-1} and one sample in both cities, Ash9 and Z1, had double high value than the recommended normal world limit. The samples collected from 10th of Ramadan city had lower concentrations of ^{40}K than the recommended normal world limit of 400 Bq kg^{-1}. While in the case of samples collected from Zagazig city, several samples had higher concentrations than this world limit. The minimum, maximum and mean values of radium equivalent content (Bqkg^{-1}), gamma absorbed dose (nGy/h), annual effective gamma dose rate (μSvyr^{-1}) and external hazard index (Bq/kg) for the most samples from 10th of Ramadan city are about half of those obtained in Zagazig samples. The computed mean dose rate for Zagazig samples is found to be less than the world average (51nGyh^{-1}), except two samples show opposite trend, as reported by[22], whereas for 10th of Ramadan samples it is found to be by far lesser than this world average (51nGyh^{-1}). Finally, our results clearly show that both cities under investigation are almost safe as far as the health hazards of radon are

concerned given in the reports issued by the[1,5,8,24], but the 10th of Ramadan city is safer than Zagazig city based on the results of the measurements of naturally radioactive concentration levels in $Bqkg^{-1}$ for ^{226}Ra, ^{238}U, ^{232}Th and ^{40}K radionuclides measured by using the finest tool HPGe gamma ray spectrometry.

In final conclusion, we conducted a study of radioactivity in a previously unknown soil area in two cities in the eastern Nile Delta. The theoretical radioisotope contents and associated radiometric parameters, calculated using Monte Carlo simulations, which include an artificial neural network, agree perfectly with experiment.

Competing interests

The authors declare no competing interests.

Fund

Open access funding provided by The Science, Technology & Innovation Funding Authority (STDF) in cooperation with The Egyptian Knowledge Bank (EKB).

Data Availability Statement: The datasets used and/or analyzed during the current study available from the corresponding author on reasonable request.

Declarations

Ethical approval

Not applicable.

Consent to participate

Not applicable.

Consent to publish

Not applicable.

References

[1] UNSCEAR, "Sources and Effects of Ionizing Radiation United Nations Scientific Committee on the Effects of Atomic Radiation, Report to the General Assembly, with Scientific Annexes VOLUME I: Sources United Nations," 2000.

[2] IAEA, *International Atomic Energy Agency - Guidelines for radioelement mapping using gamma ray spectrometry data*, no. July. 2003.

[3] M. Eisenbud and T. Gesell, *Environmental Radioactivity: From Natural, Industrial, and Military Sources*, 4th ed. Academic Press, 1997.

[4] G. F. Knoll, *Radiation Detection and Measurement*, 4th ed. John Wiley & Sons, 2010.

[5] I. C. on R. Protection, "Protection against Radon-222 at Home and at Work," *Ann. ICRP*, vol. 23, no. 2, 1993, doi: 10.1016/0146-6453(93)90003-R.

[6] IAEA, "Radiation Protection and NORM Residue Management in the Production of Rare Earths from Thorium Containing Minerals," 2011. [Online]. Available: http://www-ns.iaea.org/standards/

[7] WHO, *WHO Handbook On Indoor Radon A Public Health Perspective*. 2009.

[8] UNSCEAR, *Sources and effects of ionizing radiation : United Nations Scientific Committee on the Effects of Atomic Radiation : UNSCEAR 2008 report to the General Assembly, with scientific annexes*. United Nations, 2008.

[9] S. Gallardo, A. Querol, J. Ortiz, J. Ródenas, G. Verdú, and J. F. Villanueva, "Uncertainty analysis in environmental radioactivity measurements using the Monte Carlo code MCNP5," *Radiation Physics and Chemistry*, vol. 116, pp. 214–218, Nov. 2015, doi: 10.1016/j.radphyschem.2015.05.023.

[10] M. O. Isinkaye, P. O. Fasanmi, M. U. Khandaker, M. I. Sayyed, and M. Y. Hanfi, "Assessment of elevated levels of natural radioactivity in groundwater of artisanal gold and gemstone mining sites and estimation of concomitant risk using Monte Carlo simulation approach," *Radiation Physics and Chemistry*, vol. 235, 2025, doi: 10.1016/j.radphyschem.2025.112823.

[11] C. M. Bishop, *Neural Networks for Pattern Recognition*. Oxford University Press, 1995.

[12] S. Haykin, *Neural Networks and Learning Machines*, 3rd ed. Pearson Education, 2009.

[13] I. Goodfellow, Y. Bengio, and A. Courville, *Deep Learning*. MIT Press, 2016.

[14] Y. Ma *et al.*, "Monte Carlo simulation-based characteristics of indoor radon concentrations and exploratory probabilistic risk analysis in university buildings," *J. Environ. Radio act.*, vol. 296, May 2026, doi: 10.1016/j.jenvrad.2026.108002.

[15] B.M. Ali, Gehan Y. Mohamed, M. Al-Abyad; Activation cross sections of proton induced nuclear reactions on tungsten: Special regard to the formation of ^{186}Re. *Nuclear Physics A Volume 1045, (2024) 122833*

[16] A. Azzam, Mohamed S. Hamada, Seham, A. Said, Gehan Y. Mohamed[1], M. Al-abyad, Excitation functions for proton-induced reactions on Te and ^{nat}Ti targets: Measurements and model calculations special relevant to the ^{128}Te(p,n) ^{128}I reaction. Nuclear Physics A 999 (2020)121790

[17] A. Azzam, Gehan Y. Mohamed, M. Al-Abyad, Excitation functions and yield measurements for Proton Induced Reactions in Stainless Steel: Special relevance to Proton Activation Analysis. Applied Radiation and Isotopes 151 (2019) 166–170

[18] Yu, K. N.,Guan, Z.J., Stokes, M.J., Young, E.C.,1992. The assessment of natural radiation dose committed to Hong Kong People. J. Environ. Radioactivity 17, 31-48.

[19] Krieger, R., 181. Radioactivity of construction materials. Betonwerk Fertgteil Tech.47, 468-473.

[20] W. Z. T. Tareq, "(Artificial) neural networks," in *Decision-Making Models: A Perspective of Fuzzy Logic and Machine Learning*, 2024. doi: 10.1016/B978-0-443-16147-6.00035-9.

[21] R. Qamar and B. A. Zardari, "Artificial Neural Networks: An Overview," 2023. doi: 10.58496/MJCSC/2023/015.

[22] UNSCEAR, *Sources, Effects And Risks Of Ionizing Radiation United Nations Scientific Committee on the Effects of Atomic Radiation UNSCEAR 2024 Report to the General Assembly with Scientific Annexes*. 2024.

[23] K. Salahel Din and W. Rashed, "Assessment of norm levels and radiological hazards from petroleum extraction in the onshore oil fields, Egypt," *Radiat. Prot. Dosimetry*, vol. 194, no. 4, pp. 223–232, May 2021, doi: 10.1093/rpd/ncab099.

[24] I. A. E. Agency, "Radiation Protection and NORM Residue Management in the Production of Rare Earths from Thorium Containing Minerals," IAEA, Vienna, 2014.

[25] European Commission Radiation Protection 112, "Radiological protection principles concerning the natural radioactivity of building materials," 1999

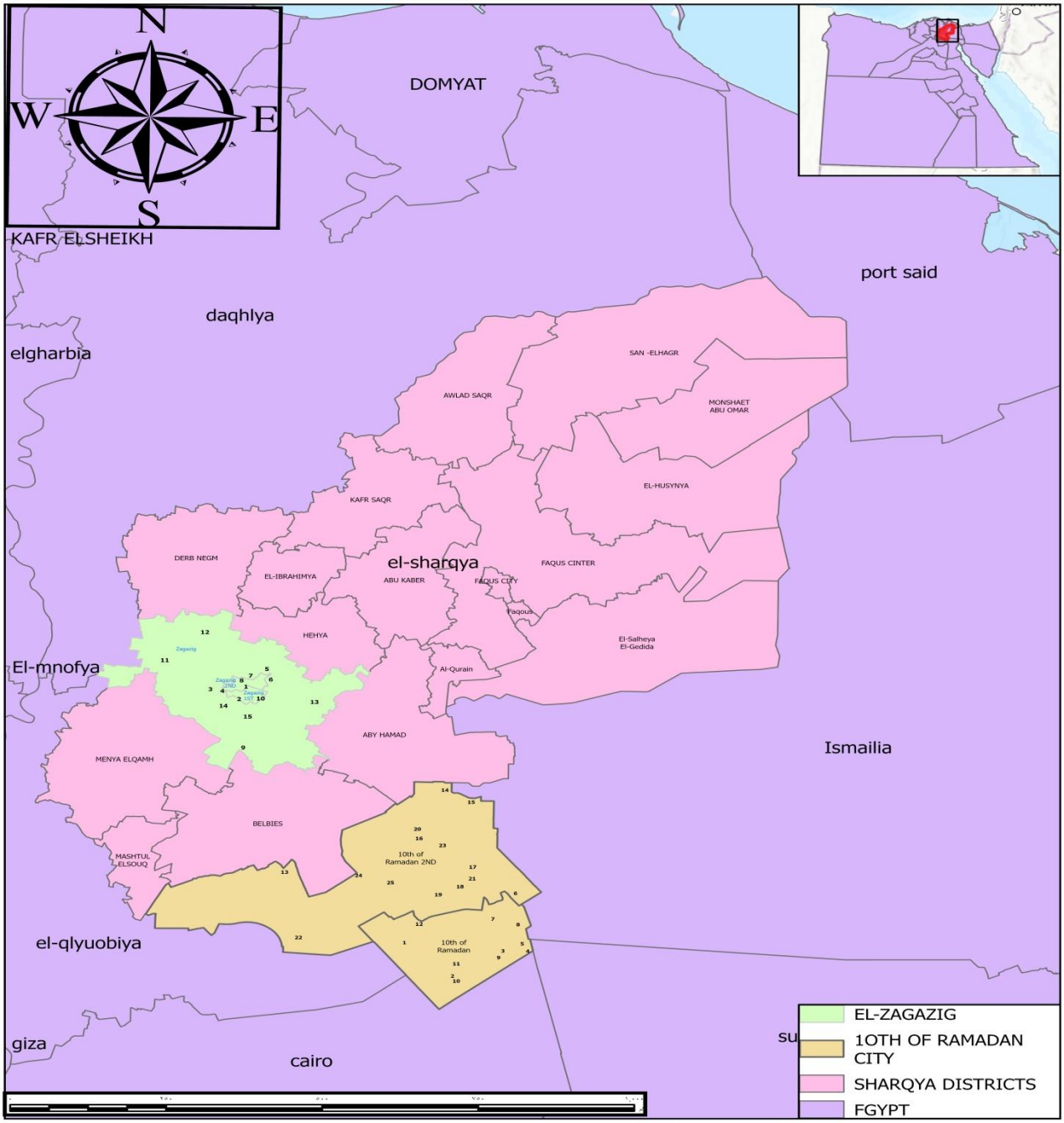

N
W
E
S
DOMYAT
KAFR ELSHEIKH
port said
daqhlya
elgharbia
SAN -ELHAGR
AWLAD SAQR
MONSHAET ABU OMAR
EL-HUSYNYA
KAFR SAQR
DERB NEGM
el-sharqya
EL-IBRAHIMYA
ABU KABER
FAQUS CITY
FAQUS CINTER
Faqous
HEHYA
El-Salheya El-Gedida
El-mnofya
Al-Qurain
ABY HAMAD
Ismailia
MENYA ELQAMH
BELBIES
MASHTUL ELSOUQ
10th of Ramadan 2ND
10th of Ramadan
el-qlyuobiya
giza
cairo
EL-ZAGAZIG
1OTH OF RAMADAN CITY
SHARQYA DISTRICTS
FGYPT

Fig. 1.

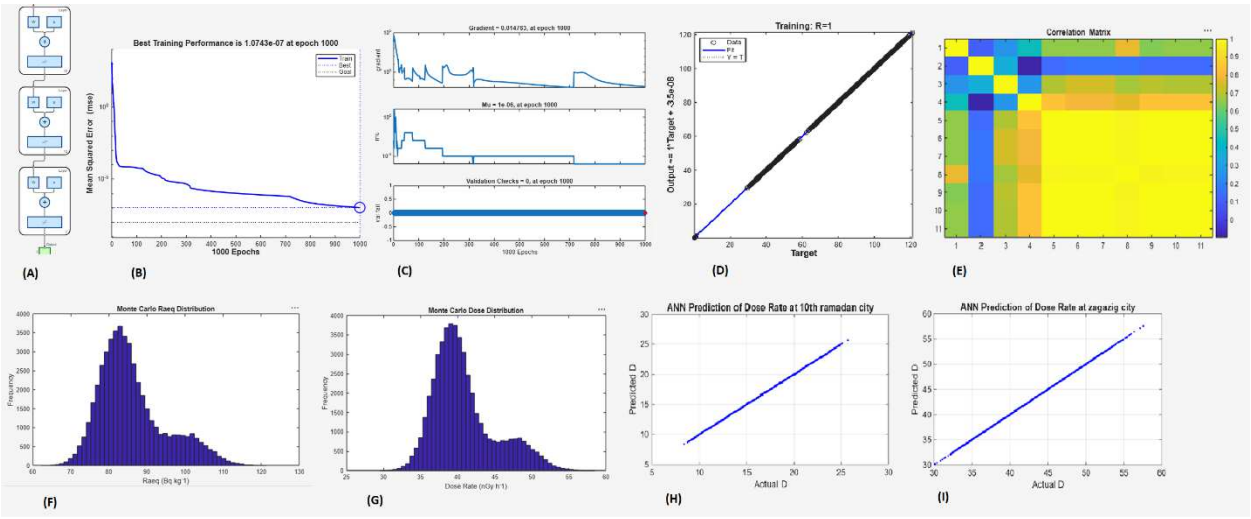


Fig. 2.

Figure Caption

Fig. 1. Map showing the study areas in (a) Benghazi and (b) Al-Marj. The numbers refer to the locations where samples were collected, as listed in Tables.

Fig. 2. Comprehensive results of the Artificial Neural Network (ANN) and Monte Carlo simulation analyses for radiological assessment: (a) architecture of the developed ANN model, (b) training performance represented by the mean squared error (MSE) curve, (c) training state showing gradient, damping factor (μ), and validation checks, (d) regression analysis between predicted and measured values, (e) correlation matrix of radionuclides and radiological hazard parameters, (f) Monte Carlo distribution of radium equivalent activity (Raeq), (g) Monte Carlo distribution of absorbed dose rate, (h) ANN prediction of dose rate for samples from 10th Ramadan City, and (i) ANN prediction of dose rate for samples from Zagazig City. The ANN achieved excellent predictive accuracy with a correlation coefficient approaching unity and a very low prediction error, while the Monte Carlo simulations confirmed the stability and reliability of the radiological risk estimates under uncertainty conditions.

Table 1 Radioactive concentration levels in $Bqkg^{-1}$ for Ra-226, U-238, Th-232 and K-40 for some radionuclides of soil samples collected from different sites in 10^{th} of Ramadan were measured by using HPGe gamma ray spectrometry. In addition to estimated parameters such as radium equivalent content ($Bqkg^{-1}$), gamma absorbed dose

Sample Code	Radioactive concentrations (Bq/kg)				Radium equivalent content (Bq/kg)	Gamma absorbed dose (nGy/h)	Annual effective gamma dose rate ($\mu Svyr^{-1}$)	External hazard index (Bq/kg)
	Ra-226	**U-238**	**Th-232**	**K-40**				
Ash†1	7.7 ± 1.6	14.4 ± 3.0	10.2 ± 2.1	156.1 ± 32.5	39.9 ± 1.2	19.3 ± 5.6	23.7 ± 6.9	0.111 ± 0.032
Ash2	8.1 ± 1.7	15.3 ± 3.2	10.4 ± 2.1	133.4 ± 27.8	39.5 ± 1.1	18.9 ± 5.4	23.7 ± 6.6	0.109 ± 0.031
Ash3	9.9 ± 2.1	17.5 ± 3.6	12.4 ± 2.6	155.8 ± 32.7	46.1 ± 1.3	22.1 ± 7.3	23.7 ± 9.0	0.127 ± 0.043
Ash4	6.6 ± 1.4	12.2 ± 3.0	10.7 ± 2.2	103.4 ± 21.1	34.7 ± 1.0	16.4 ± 5.0	23.7 ± 6.1	0.096 ± 0.010
Ash5	11.9 ± 0.5	34.9 ± 7.2	14.0 ± 0.6	181.6 ± 10.3	67.5 ± 1.5	32.1 ± 3.9	23.7 ± 4.8	0.186 ± 0.024
Ash6	8.7 ± 2.0	16.0 ± 8.3	8.9 ± 2.1	135.7 ± 29.1	38.2 ± 1.1	18.4 ± 6.2	23.7 ± 7.6	0.106 ± 0.034
Ash7	8.1 ± 1.7	13.3 ± 8.6	8.5 ± 1.8	110.6 ± 23.5	33.2 ± 1.0	15.9 ± 5.9	23.7 ± 7.2	0.092 ± 0.035
Ash8	11.3 ± 0.6	27.8 ± 7.9	12.2 ± 0.7	172.5 ± 10.3	57.3 ± 1.4	27.4 ± 4.3	33.6 ± 5.3	0.158 ± 0.026
Ash9	5.6 ± 1.2	53.2 ± 14.6	6.8 ± 1.5	99.3 ± 20.9	69.9 ± 0.8	32.8 ± 8.1	40.2 ± 9.9	0.191 ± 0.050
Ash10	8.5 ± 0.4	17.9 ± 5.4	9.8 ± 0.4	128.4 ± 7.3	40.9 ± 1.1	19.5 ± 2.9	23.9 ± 3.6	0.113 ± 0.018
Ash11	10.4 ± 2.3	18.8 ± 6.1	10.7 ± 2.3	136.9 ± 29.5	43.7 ± 1.2	20.9 ± 5.4	25.6 ± 6.6	0.121 ± 0.024
Ash12	9.4 ± 1.9	30.3 ± 8.2	10.1 ± 2.1	139.0 ± 28.9	54.4 ± 1.2	25.9 ± 6.1	31.8 ± 7.5	0.150 ± 0.036
Ash13	10.5 ± 0.5	31.8 ± 7.6	10.1 ± 0.5	129.9 ± 7.5	55.3 ± 1.2	26.2 ± 3.9	32.1 ± 4.8	0.152 ± 0.024
Ash14	6.6 ± 0.7	12.2 ± 6.1	8.8 ± 0.7	122.3 ± 8.5	33.4 ± 1.0	16.1 ± 3.4	19.7 ± 4.2	0.093 ± 0.017
Ash15	11.8 ± 0.6	18.4 ± 7.5	13.3 ± 0.6	148.9 ± 8.9	47.9 ± 1.4	22.8 ± 4.0	28.0 ± 4.9	0.132 ± 0.025

Ash16	11.6 ± 0.7	23.1 ± 8.6	12.5 ± 0.7	140.4 ± 9.0	50.8 ± 1.4	24.1 ± 4.5	29.6 ± 5.5	0.140 ± 0.028
Ash17	10.3 ± 0.4	14.6 ± 4.7	12.1 ± 0.5	138.2 ± 7.8	41.6 ± 1.3	19.8 ± 2.7	24.3 ± 3.3	0.115 ± 0.016
Ash18	11.0 ± 0.4	20.4 ± 5.0	14.1 ± 0.5	146.7 ± 8.2	50.8 ± 1.4	24.1± 2.8	29.6 ± 3.4	0.140 ± 0.017
Ash19	8.0 ± 0.4	20.4 ± 5.2	9.2 ± 0.4	162.2 ± 9.1	44.9 ± 1.1	21.7 ± 2.9	26.6 ± 3.6	0.124 ± 0.018
Ash20	7.8 ± 0.4	13.0 ± 5.0	8.0 ± 0.4	121.6 ± 6.9	33.0 ± 1.0	15.9 ± 2.7	19.5 ± 3.3	0.091 ± 0.016
Ash21	8.6 ± 0.6	22.3 ± 8.1	10.3 ± 0.6	144.6 ± 9.2	47.2 ± 1.2	22.6 ± 4.3	27.7 ± 5.3	0.130 ± 0.026
Ash22	10.1 ± 0.4	22.1 ± 5.0	11.7 ± 0.4	144.8 ± 8.1	48.9 ± 1.2	23.3 ± 2.8	28.6 ± 3.4	0.135 ± 0.017
Ash23	8.5 ± 0.4	27.6 ± 5.2	10.8 ± 0.4	131.2 ± 7.4	52.3 ± 1.3	24.8 ± 2.8	30.4 ± 3.4	0.144 ± 0.017
Ash24	10.2 ± 0.7	20.7 ± 8.8	11.6 ± 0.7	148.4 ± 9.1	47.6 ± 1.1	22.7 ± 4.4	27.8 ± 5.4	0.131 ± 0.026
Ash25	9.7 ± 0.5	11.1 ± 5.6	11.4 ± 0.5	139.2 ± 8.1	37.1 ± 1.3	17.8 ± 3.1	21.8 ± 3.8	0.103 ± 0.019

Table 2

Radioactive concentration levels (Bq kg^{-1}), radium equivalent content (Bq kg^{-1}), gamma absorbed dose (nGyh^{-1}), annual effective dose equivalent (μSv) and external hazard indexes (Bq kg^{-1}) for some radionuclides in soil samples were measured by using HPGe gamma ray spectrometry. Z stands for Zagazig.

Sample Code	Radioactive concentrations (Bq/kg)				Radium equivalent content (Bq/kg)	Gamma absorbed dose (nGy/h)	Annual effective gamma dose rate (μ Svyr^{-1})	External hazard index (Bq/kg)
	Ra-226	**U-238**	**Th-232**	**K-40**				
Z1	18.3 ± 1.2	52.4 ± 18.9	27.0 ± 1.7	372.5 ± 22.7	117.1 ± 5.3	56.1 ± 10.2	56.1 ± 10.2	0.323 ± 0.014
Z2	21.4 ± 0.8	29.8 ± 9.2	28.2 ± 1.1	498.0 ± 26.9	105.1 ± 4.5	51.6 ± 5.8	51.6 ± 5.8	0.293 ± 0.012
Z3	18.0 ± 0.7	15.7 ± 9.4	23.2 ± 1.1	389.6 ± 21.4	76.1 ± 4.0	37.5 ± 1.9	46.0 ± 2.3	0.213 ± 0.011
Z4	16.5 ± 0.7	24.6 ± 9.6	25.4 ± 1.0	386.0 ± 21.1	87.9 ± 3.8	42.8 ± 1.9	52.5 ± 2.3	0.245 ± 0.010
Z5	17.6 ± 1.3	26.3± 10.6	23.3 ± 1.2	392.3 ± 21.9	87.1 ± 4.7	42.6 ± 6.3	52.2 ± 7.7	0.243 ± 0.013
Z6	17.9 ± 0.8	18.9 ± 10.3	28.1 ± 1.3	443.4 ± 24.4	90.2 ± 4.5	44.2 ± 2.2	54.2 ± 2.7	0.252 ± 0.012
Z7	18.0 ± 1.1	20.3 ± 10.8	24.7 ± 1.7	451.1 ± 26.0	87.2 ± 5.5	43.1 ± 6.9	52.9 ± 8.5	0.244 ± 0.015
Z8	19.3 ± 1.4	21.8 ± 11.6	24.2 ± 1.9	457.8 ± 27.3	88.5 ± 6.3	43.8 ± 3.0	53.7 ± 3.7	0.248 ± 0.017
Z9	18.2 ± 0.8	35.9 ± 9.2	24.8 ± 1.1	327.1 ± 18.3	94.2 ± 3.7	45.2 ± 1.8	55.4 ± 2.2	0.260 ± 0.010
Z10	17.0 ± 1.2	47.8 ±10.4	21.9 ± 1.6	344.6 ± 21.9	103.2 ± 5.1	49.7 ± 2.5	61.0 ± 3.1	0.285 ± 0.014
Z11	17.6 ± 0.7	41.3 ± 10.1	24.7 ± 1.1	317.9 ± 17.5	98.9 ± 3.6	47.3 ± 1.7	58.0 ± 2.1	0.273 ± 0.010

† Stands for Ashir min Ramadan (10th of Ramadan).

1Z12	17.8 ± 0.6	21.6 ± 8.2	20.2 ± 0.9	305.7 ± 16.8	71.9 ± 3.1	34.9 ± 1.5	42.8 ± 1.8	0.200 ± 0.008
2Z13	19.3 ± 0.8	28.7 ± 10.6	25.6 ± 1.1	385.3 ± 21.2	92.2 ± 4.0	44.8 ± 1.9	54.9 ± 2.3	0.256 ± 0.011
Z14	15.8 ± 0.7	43.5 ± 11.1	20.4 ± 1.1	356.1 ± 19.4	97.6 ± 3.7	47.3 ± 1.8	58.0 ± 2.2	0.270 ± 0.010
3Z15	13.8 ± 0.7	39.9 ± 11.5	20.0 ± 1.1	417.9 ± 23.1	97.8 ± 4.1	48.0 ± 2.0	58.9 ± 2.5	0.272 ± 0.011

	Radioactive concentrations (Bq/kg)							
	10th of Ramadan				Zagazig			
	Ra-226	U-238	Th-232	K-40	Ra-226	U-238	Th-232	K-40
Minimum	5.6 ± 0.4	11.1 ± 3.0	6.8 ± 0.4	99.3 ± 6.9	13.8 ± 0.6	15.7 ± 8.2	20.0 ± 0.9	305.7 ± 16.8
Maximum	11.9 ± 2.3	53.2 ± 14.6	14.1 ± 2.6	181.6 ± 32.7	21.4 ± 1.4	52.4 ± 18.9	28.2 ± 1.9	498.0 ± 27.3
Range	6.3 ± 1.9	42.1 ± 11.6	7.3 ± 2.2	82.3 ± 25.8	7.6 ± 0.8	36.7 ± 10.7	8.2 ± 1.0	192.3 ± 10.5
Mean	9.4 ± 0.6	18.8 ± 6.1	10.7 ± 0.6	139.0 ± 9.1	17.9 ± 0.8	28.7 ± 10.4	24.7 ± 1.1	386.0 ± 21.9
Standard deviation	1.7 ± 0.6	9.1 ± 2.5	1.8 ± 0.7	18.8 ± 9.4	1.6 ± 0.2	11.1 ± 2.3	2.6 ± 0.3	53.8.0 ± 3.1

Table 3 Statistical of radioactive concentrations of ^{226}Ra, ^{238}U, ^{222}Th and ^{40}K, radium equivalent content, gamma absorbed dose, annual effective gamma dose rate and external hazard index of both cities 10th of Ramadan and Zagazig.

Radium equivalent content (Bq kg^{-1})		Gamma absorbed dose (nGy/h)		Annual effective gamma dose rate (μSvyr^{-1})		External hazard index (Bq/kg)	
10th of Ramadan	Zagazig	10th of Ramadan	Zagazig	10th of Ramadan	Zagazig	10th of Ramadan	Zagazig
33.0 ± 0.8	71.9 ± 3.1	15.9 ± 2.7	34.9 ± 1.5	19.5 ± 3.3	42.8 ± 1.8	0.09 ± 0.01	0.20 ± 0.01
69.9 ± 1.5	117.1 ± 6.3	32.8 ± 8.1	56.1 ± 10.2	40.2 ± 9.9	61.0 ± 10.2	0.19 ± 0.05	0.32 ± 0.02
36.9 ± 0.7	45.2 ± 3.2	16.9 ± 5.4	21.2 ± 8.7	20.7 ± 6.6	18.2 ± 8.4	0.10 ± 0.04	0.12 ± 0.01
46.1 ± 1.2	92.2 ± 4.1	22.1 ± 4.3	44.8 ± 2.0	25.6 ± 5.3	54.2 ± 2.5	0.13 ± 0.02	0.26 ± 0.01
9.6 ± 0.2	10.9 ± 0.8	4.5 ± 1.5	5.1 ± 2.5	4.6 ± 1.8	4.6 ± 2.6	0.03 ± 0.01	0.03 ± 0.00

Table 4. Comparison Between the measured and Monte Carlo simulated radiological parameters for soil samples collected from ^{10}th of Ramadan city and Zagazig city.

Radiological parameter	^{10}th of Ramadan city			Zagazig city			Recommended limit	Ref.
	Experimental measurements	Monte Carlo Simulation	MSE (%)	Experimental measurements	Monte Carlo Simulation	MSE (%)		
Ra-226 (Bq kg^{-1})	9.26 ± 1.71	9.71 ± 0.96	0.048	17.77 ± 1.70	17.59 ± 1.77	0.010	35	[1,22]
U-238 (Bq kg^{-1})	21.17 ± 9.31	11.10 ± 1.10	0.476	31.23 ± 11.47	26.27 ± 2.61	0.159	35	
Th-232 (Bq kg^{-1})	10.74 ± 1.83	11.40 ± 1.14	0.061	24.11 ± 2.65	23.27 ± 2.32	0.035	30	
K-40 (Bq kg^{-1})	138.80 ± 19.20	139.13 ± 13.77	0.002	389.69 ± 55.71	392.20 ± 39.27	0.006	400	
Dose (nGy h^{-1})	16.56 ± 2.45	17.17 ± 1.00	0.037	39.02 ± 3.89	38.54 ± 2.31	0.012	59–60	
Ra_{eq} (Bq kg^{-1})	35.31 ± 5.29	36.72 ± 2.18	0.040	82.25 ± 8.08	81.07 ± 4.84	0.014	370	
H_{ex}	0.095 ± 0.014	0.099 ± 0.006	0.040	0.222 ± 0.022	0.219 ± 0.013	0.015	< 1	
H_{in}	0.120 ± 0.019	0.125 ± 0.007	0.042	0.270 ± 0.025	0.267 ± 0.016	0.014	< 1	
AED_{out} (mSv y^{-1})	0.020 ± 0.003	0.021 ± 0.001	0.039	0.048 ± 0.005	0.047 ± 0.003	0.013	0.07	
AED_{in} (mSv y^{-1})	0.081 ± 0.012	0.084 ± 0.005	0.037	0.191 ± 0.019	0.189 ± 0.011	0.012	0.41	
I gamma	0.262 ± 0.039	0.272 ± 0.016	0.037	0.619 ± 0.062	0.612 ± 0.037	0.013	< 1	[25]